

FACILITY FOR:

(ACCESSION NUMBER)

34

(PAGES)

CR-68489

(NASA CR OR TMX OR AD NUMBER)

(THRU)

(CODE)

(CATEGORY)

Lifetimes and g_J Factors in Excited States of Chromium.Hyperfine Structure of Cr^{53*} H. Bucka,[†] B. Budick,[‡] R.J. Goshen,** and S. MarcusColumbia Radiation Laboratory,Columbia University, New York, New York 10027

ABSTRACT

36096

The 7P terms of two excited chromium configurations have been studied by the techniques of level crossing and double resonance spectroscopy. The lifetimes of the J levels of the two terms were found by observation of the Hanle effect to be $(3.34 \pm 0.5) \times 10^{-8}$ sec and $(6.51 \pm 0.9) \times 10^{-9}$ sec for $(3d^5 4p)^7P_4$ and $(3d^4 4s 4p)^7P_4$ respectively. g_J values for the three J levels of the $(3d^5 4p)^7P$ term were also determined; $g(J=4) = 1.7512(3)$, $g(J=3) = 1.9178(2)$, and $g(J=2) = 2.3351(3)$.

*This work was supported in part by the National Aeronautics and Space Administration under Grant NsG-360 and in part by the Joint Services Electronics Program (U.S. Army, U.S. Navy, and U.S. Air Force) under Contract DA-36-039 SC-90789.

[†]Present address: Institut für Kernphysik an der Technischen Universität, Berlin, West Germany.

[‡]Present address: Microwave Laboratory, Hebrew University, Jerusalem, Israel.

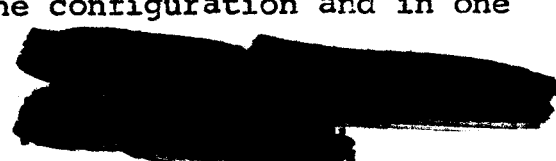
**Present address: Hudson Laboratories, Columbia University, Dobbs Ferry, New York.

For the purpose of studying core polarization in chromium, measurements were made of the magnetic hyperfine constants in both configurations. For $3d^5 4p$, $|a(J=4)| = 11.6 \pm 0.15$ Mc, $|a(J=3)| \leq 1.5 \pm 2.0$ Mc, $|a(J=2)| = 26.16 \pm 0.10$ Mc, and for $3d^4 4s 4p$, $|a(J=3)| = 70.4 \pm 2.6$ Mc.

INTRODUCTION

The techniques of level crossing spectroscopy and optical double resonance have been applied in a study of the electronic and nuclear properties of the isotopes of chromium. This is the first experiment in which the excited states of a transition metal have been studied by radio-frequency methods in the case of the free atom. The nuclear magnetic moment of Cr^{53} has been determined to high precision by NMR.⁽¹⁾ The quadrupole moment has been measured roughly in an ENDOR experiment.⁽²⁾ The uncertainty in this result arises since the interpretation of the data obtained in the ENDOR technique necessarily presumes a knowledge of the crystal field environment. No information concerning the quadrupole interaction was gained in our experiment due to the large line-widths associated with the excited states.

We expected that polarization of the core electrons by the external d electrons would contribute significantly to the hyperfine interaction. Measurements of the hyperfine constants in three J levels of one configuration and in one



J level of an interacting configuration were made to study this phenomenon more closely. The effect was observed as was the effect of configuration mixing. The interpretation of the data in terms of core polarization is given in the following paper.⁽³⁾

THEORY

The low-lying energy levels of chromium are shown in Fig. 1. The ground state has a half-filled d shell and a single s electron. Its hyperfine structure has been measured in an atomic beam experiment by Goodman and Childs.⁽⁴⁾ No quadrupole interaction is expected in the 7S_3 state. The six valence electrons form two low-lying odd configurations $(3d)^5 4p$ and $(3d)^4 4s 4p$ connected to the ground state via s-p and d-p transitions respectively. Two identical Russell-Saunders states can be formed from these configurations, both designated as $^7P_{2,3,4}$. The wavelengths for both multiplets are in the convenient ranges 4250-4300 Å and 3570-3610 Å respectively.

Measurements of the lifetimes of both excited multiplets were made by observing the Hanle or zero-field level crossing effect. The theory for this effect has been treated both classically⁽⁵⁾ and quantum mechanically⁽⁶⁾ and will not be reviewed here. Our observations consist of intensity measurements of the light scattered at 90° to the incident light beam. The intensity is given as a function of magnetic field by⁽⁵⁾

$$I = \frac{C}{2} \left[1 - \frac{\Gamma^2}{\Gamma^2 + 4\gamma^2 H^2} \right] \quad (1)$$

where Γ is the reciprocal of the mean life of the excited state, γ is the gyromagnetic ratio, and C is an arbitrary constant relating to the incident light intensity, the experimental geometry, and the number of scatterers. The line shape as a function of H is an inverted Lorentzian with a full width at half-maximum equal to Γ . The half-maximum occurs at a field value $H_{1/2}$ for which $4\gamma^2 H_{1/2}^2 = \Gamma^2$. Substituting $\Gamma = 1/\tau$, $\gamma = g_J(\mu_O/\hbar)$, we obtain

$$\frac{1}{\tau} = 2g_J \frac{\mu_O}{\hbar} H_{1/2} \text{ sec}^{-1} \quad (2)$$

An unsuccessful attempt was made to observe hyperfine structure level crossings. Consequently the experiments on the g_J values and hyperfine structure were performed with the technique of high field double resonance.⁽⁷⁾ The Hamiltonian appropriate to the case where the field is strong enough to decouple I and J has the form

$$\begin{aligned} \mathcal{H} = & g_J \mu_O m_J H + g_I \mu_O m_I H + a m_I m_J \\ & + \frac{b}{4} \frac{[3m_J^2 - J(J+1)][3m_I^2 - I(I+1)]}{IJ(2I-1)(2J-1)} \end{aligned} \quad (3)$$

where a and b are the nuclear magnetic dipole and electric quadrupole hyperfine constants. The radio frequency required to induce transitions of the type $\Delta m_J = \pm 1$, $\Delta m_I = 0$ is

$$h\nu = g_J \mu_O H + a m_I + \frac{b}{4} \frac{(6m_J - 3)}{J(2J - 1)} \frac{[3m_I^2 - I(I + 1)]}{I(2I - 1)} \quad (4)$$

For the even isotopes of chromium ($I = 0$), which are 90% abundant in a natural sample, the last two terms are absent. The remaining term enables one to measure g_J precisely. With a magnetic interaction present the transition frequency is shifted from the central maximum, and resonances appear at $\pm \frac{1}{2}a$, $\pm \frac{3}{2}a$... for the case of a half-integral spin. Thus the magnetic constant can be determined directly. The quadrupole moment is small, ⁽²⁾ and in any case splits each of the peaks symmetrically about its center, if we assume that $a \gg b$.

The change in polarization of the fluorescent light due to transitions in each of the J levels has been calculated assuming complete saturation of the radio-frequency resonance. The π component of the scattered radiation was expected to be reduced by 30, 43, and 5% for the levels $J = 4, 3, 2$ respectively. This was consistent with observations.

EXPERIMENTAL APPARATUS AND PROCEDURE

With the exception of two modifications, the apparatus is identical to that used for the measurement of the fine structure in the 3P state of lithium. ⁽⁸⁾ The atomic beam is produced by an oven heated by electron bombardment. Ovens of molybdenum or tantalum in the form of cylinders closed at one end were placed at the center of a 6-mil tungsten wire winding.

A voltage of +1500 V applied to the oven from a current stabilized power supply (Kepco 1520B) and a current of about 2 A through the filament were sufficient to raise the oven temperature so that a working vapor pressure of chromium was attained. Natural chromium in the form of cylinders 0.3 in. in diameter and 0.5 in. long fitting smoothly into the oven was used in the lifetime and g_J -value experiments. Powder samples of metallic chromium-53 enriched to 82% or higher were used to make the hyperfine structure measurements. No serious attempt was made to collimate the atomic beam. A boron nitride plug for the purpose of preventing bombardment electrons from escaping into the radio-frequency field region and a grounded molybdenum heat shield provided some collimation.

The source of resonance radiation was a Schüller-type hollow cathode. Details of the lamp construction, operation, and performance have been published.⁽⁹⁾ It was essential to operate the lamp at a very low residual gas pressure (about 10^{-5} Torr) in order to produce intense chromium light. The relative intensities of the spectral lines of the $(3d^5 4p)^7 P \rightarrow (3d^5 4s)^7 S$ triplet were $I_{4-3} : I_{3-3} : I_{2-3} = 4.0 : 2.5 : 1.5$ using the 4226-Å filter described in the following paragraph.

A Dumont No. 7664 photomultiplier was used to detect the fluorescence from both triplets. For the Hanle effect measurements a narrow-band interference filter centered at

4226 Å favored the $J = 4$ transition at 4254 Å, while a broad-band color filter was used with the triplet of the d^4sp configuration. In the double resonance work the first filter was replaced by a filter peaked at 4258 Å whose full width at half-maximum was 16 Å.

The radio-frequency coil is shown in Fig. 3. The current runs down a septum in the center and back along the outside. Wire mesh admits light and atoms to the transition region while it prevents rf leakage. The g_J experiments were performed at high field and high frequencies. A high-power magnetron (Litton L3505) operating at about 4 kMc served as a rf source. Measurements of the hyperfine structure of the levels of the d^5p configuration were made with the use of a cavity-tuned Airborne Instruments Co. power oscillator type 124A operating with a 2C39 UHF triode. A fixed frequency high-power magnetron (Raytheon QK390), operating at about 2460 Mc/sec, was used to study the hyperfine structure of the 7P_3 state of the d^4sp configuration. Lock-in detection was used to increase the signal-to-noise ratio, and all three frequency sources were amplitude modulated at 30 cps.

EXPERIMENTAL RESULTS

(a) Lifetimes

Hanle patterns observed in the resonance radiation from the 7P terms of both the $3d^5p$ and $3d^4s4p$ configurations are

shown in Fig. 3. These recorder traces are dispersion-type curves which are the derivatives of the Lorentzian lines.

They are obtained when the static magnetic field is modulated by an alternating field of small amplitude and low frequency for the purpose of lock-in detection. The ideal modulation amplitude for appreciable signal with small modulation broadening is about one-third the half-width of the resonance.

The lifetime may be deduced from the linewidth with the aid of Eq. (2) which can be written

$$\tau = \frac{1}{g_J \frac{\mu_0}{\hbar} \Delta H_{1/2}} \quad (5)$$

where $\Delta H_{1/2}$ is the full-width at half-maximum of the actual Lorentzian line shape. The determination of $\Delta H_{1/2}$ is complicated by the fact that each curve is a superposition of level crossings in all three J levels. Since the lifetimes of the J levels of the same multiplet are nearly equal, Eq. (5) implies that the largest $\Delta H_{1/2}$ will occur for the transition whose upper level has the smallest g_J factor. [In this case $g_J(^7P_4) = 1.75$.] The radiation rates as calculated from the Breit formula⁽⁵⁾ are in the ratio $R_{4 \leftarrow 3} : R_{3 \leftarrow 3} : R_{2 \leftarrow 3} = 99:147:8$. The lamp output intensity measurements described above also favor the J = 4 and J = 3 levels. The 4254-Å line corresponding to the $^7P_4 \rightarrow ^7S_3$ transition was favored by the interference

filter used in the $3d^5 4p$ measurement. These considerations suggest that the width of the observed pattern may be attributed to the ${}^7P_4 \rightarrow {}^7S_3$ transition. The presence of even a significant signal from the ${}^7P_3 \rightarrow {}^7S_3$ transition introduces an error which is small compared to the experimental precision. Light from the ${}^7P_2 \rightarrow {}^7S_3$ transition would introduce considerable error because of the large difference between $g_J(J=4)$ and $g_J(J=2)$, but the results for the radiation rates preclude such an effect.

The best data yield 1.13 G and 5.80 G for the peak-to-trough separations of the Hanle dispersion patterns of the $(3d^5 4p) {}^7P_4$ and $(3d^4 4s 4p) {}^7P_4$ levels respectively. A factor of $\sqrt{3}$ must be included to convert these separations to the full half-widths at half-maximum of the integrated Lorentzian line. We have

$$\begin{aligned}\Delta H_{1/2}(3d^5 4p) &= 1.13 \times \sqrt{3} = 1.95 \text{ G} \\ \Delta H_{1/2}(3d^4 4s 4p) &= 5.80 \times \sqrt{3} = 10.0 \text{ G} \quad .\end{aligned}\tag{6}$$

The field measurements were made with a Hall probe (Bell gaussmeter) since the absolute fields were too low to obtain usable proton resonance signals. The gaussmeter is sufficiently accurate for the lifetime determination (better than 1%). The magnetic field sweep was studied as a function of magnet current since the magnet power supply was not well regulated near

zero field. Only a very slight departure from linearity was found in the wings of the Hanle pattern. The resulting lifetimes from Eq. (5) are

$$\begin{aligned}\tau[(3d^5 4p)^7 P_4] &= (3.34 \pm 0.5) \times 10^{-8} \text{ sec} \\ \tau[(3d^4 4s 4p)^7 P_4] &= (6.51 \pm 0.9) \times 10^{-9} \text{ sec.}\end{aligned}\quad (7)$$

The limits of error allow for the presence of field inhomogeneity broadening and coherence narrowing. These effects were not thoroughly investigated.

(b) g_J Values

For a spin zero isotope Eq. (4) is simply

$$h\nu = g_J \mu_O H \quad . \quad (8)$$

The curves shown in Fig. 4 were taken at 1600 G and approximately 4 kMc. Markers indicate the resonance frequency in kc/sec for protons in a mineral oil sample. The transition frequency is the 20th harmonic of the frequency listed at the top of each curve. Both proton resonance and transition frequencies were measured with Hewlett-Packard model 5243L frequency counters. The small error introduced by the time constant of the sweep was eliminated by averaging data taken in both sweep directions.

The final result for g_J in each J level is tabulated in Table I together with the pure L-S coupling value and a

determination made from earlier optical spectroscopic work. ⁽¹⁰⁾

The radio-frequency and optical values are in good agreement.

(c) Hfs Constants in $(3d^5 4p)^7 P_{2,3,4}$ and $(3d^4 4s 4p)^7 P_3$

The presence of the hyperfine interaction in the odd-A isotope Cr^{53} ($I=3/2$) produces a splitting of the $g_J \mu_B H$ peak into four equally spaced peaks whose separation is just the a value, provided the magnetic field completely uncouples I and J . The results of an early run in the $J = 3$ and $J = 4$ states with a sample enriched to 82% odd-isotope are shown in Fig. 5. The patterns were obtained at 840 Mc/sec. The $J = 4$ pattern is indeed a superposition of four peaks augmented by the $I = 0$ resonance as is borne out by Fig. 6. This result was obtained using a 99% enriched sample. The $J = 3$ state, however, shows no hyperfine structure, a result that remained unchanged in subsequent experiments.

If one assumes that the outer p electron alone is involved in the hyperfine interaction, the magnetic constants are predicted to be in the ratio $|a(4)| : |a(3)| : |a(2)| = 81:140:101$. The $J = 3$ level is expected to have the largest hyperfine splitting of the three levels of $(3d^5 4p)^7 P$, but virtually no splitting is observed. It is as though the hyperfine interaction had been quenched in that level.

Figure 7 shows a sample of data taken in the $J = 2$ state at 770.8 Mc/sec. The four peaks are quite well resolved, in contrast to the $J = 4$ resonance in Fig. 6. The $J = 2$ peaks, however, are actually not quite uniformly spaced because of incomplete decoupling of I and J. The first-order perturbation result of Eq. (3) is inadequate for the precision of the measurement. Second-order theory is necessary for this case. From the off-diagonal matrix elements of $a\vec{I} \cdot \vec{J}$ in the $m_I m_J$ representation we derive the following transition frequencies for $\Delta m_I = 0$ resonances:

$$\begin{aligned}
 h\nu(m_I = 3/2) &= g_J \mu_O H_{3/2} + \frac{3}{2}a + \frac{3}{4} \frac{a^2}{g_J \mu_O H_{3/2}} , \\
 h\nu(m_I = 1/2) &= g_J \mu_O H_{1/2} + \frac{1}{2}a + \frac{7}{4} \frac{a^2}{g_J \mu_O H_{1/2}} , \\
 h\nu(m_I = -1/2) &= g_J \mu_O H_{-1/2} - \frac{1}{2}a + \frac{7}{4} \frac{a^2}{g_J \mu_O H_{-1/2}} , \\
 h\nu(m_I = -3/2) &= g_J \mu_O H_{-3/2} - \frac{3}{2}a + \frac{3}{4} \frac{a^2}{g_J \mu_O H_{-3/2}} .
 \end{aligned} \tag{9}$$

For simplicity one may set $H_{3/2} = H_{1/2} = H_{-1/2} = H_{-3/2}$ in the last term of these equations, thereby neglecting a higher order term. Then the second and third equations give

$$\left| \frac{a}{h} \right| = \frac{g_J \mu_O}{h} (H_{-1/2} - H_{1/2}) , \tag{10}$$

while the first and fourth equations yield

$$\left| \frac{a}{h} \right| = \frac{1}{3} \frac{g_J \mu_O}{h} (H_{-3/2} - H_{3/2}) . \tag{11}$$

The average value for $(H_{-1/2} - H_{1/2})$ is 34.18 kc in units of the proton frequency while $(H_{-3/2} - H_{3/2})_{av}$ is 101.91 kc. Equation (10) then gives $|a| = 26.24$ Mc while from Eq. (11) we find $|a| = 26.08$ Mc. Taking the mean of these two determinations, our final result for the magnetic interaction constant is $|a(J=2)| = 26.16 \pm 0.10$ Mc. This result was used to check the adequacy of the second-order approximation by calculating the expected field values for the peaks. All measured and predicted positions were found to be in almost perfect agreement.

The first-order perturbation theory is sufficient for determining the splitting in the hfs pattern of the $J = 4$ state since the hyperfine interaction is considerably smaller and the decoupling of I and J more complete than in the $J = 2$ state. The magnetic interaction constant is obtained by fitting the data curves to four equally spaced Lorentzian-shaped lines (Fig. 6 illustrates this procedure). We varied the amplitude, width, and spacing of the four lines (keeping the amplitude and width of all peaks the same relative to one another) until their envelope coincided with the observed resonances. $|a(J=4)|$ is given directly to first order by the separation of adjacent lines. The final value obtained by this process is $|a(J=4)| = 11.6 \pm 0.15$ Mc.

It is clearly impossible to give anything better than an upper limit to $|a(J=3)|$. A careful study of the broadening of a set of data curves similar to Fig. 5 leads to the conclusion that $|a(J=3)| \leq 1.5 \pm 2.0$ Mc.

Double resonance work in the $(3d^4 4s 4p)^7P$ term was hampered by the severe radio-frequency power requirements imposed by the short lifetime. Only the $J = 3$ state Zeeman transitions were of sufficient intensity to be of use. Unfortunately, the linewidths of these transitions are large and the g_J value too close to that of a free electron. As a result, all four hyperfine peaks could not be observed before an enormous electron signal swamped the desired signal. This difficulty was reduced by working at higher fields where the small difference in g factors permits greater resolution, by improving the vacuum so less residual gas was available for ionization and excitation by the electrons, and by carefully tuning the power into the transition region. With these improvements two well resolved peaks and the beginning of a third could be reproduced and studied. Second-order terms of the type appearing in Eq.(9) were included, and the a value was calculated by successive approximations. The final value is $|a(^7P_3)| = 70.4 \pm 2.6$ Mc.

Only absolute magnitudes for the hyperfine constants have been determined. The sign of $a(J)$ cannot be ascertained

with the arrangement of polarizers employed for the measurements. It would be necessary to excite with $\sigma+$ or $\sigma-$ radiation to obtain information about the signs.⁽¹¹⁾ Unfortunately, the physical characteristics of the iron magnet preclude the performance of an experiment with pure $\sigma+$ or pure $\sigma-$ components.

DISCUSSION

The values for the lifetimes are summarized in Table II together with the results of optical spectroscopy measurements.⁽¹²⁾ Values for the oscillator strengths given by Corliss and Bozmann are converted to lifetimes by the relation

$$f\tau = 1.499 \frac{g_2}{g_1} \lambda^2, \quad (12)$$

where g_2 and g_1 are the statistical weights of the upper and lower levels respectively, and f is the oscillator strength for the line in absorption.⁽¹³⁾ A theoretical value for $\tau[(3d^5 4p)^7 P_4]$, calculated by the method of Bates and Damgaard, is included in the table for comparison with the experimental results. The Hanle effect lifetimes are in agreement with the values obtained by optical spectroscopy, although the precision of the latter measurements is poor. On the other hand, there is only order of magnitude agreement with the calculated value, probably due to a failure of the Coulomb approximation as one goes to more complex spectra.

The g_J values have been computed from the transition frequencies of the spin zero isotopes assuming the validity of Eq. (8). However, the Zeeman operator possesses matrix elements off-diagonal in J which lead to a quadratic field term in the expression for the energy of a particular Zeeman level. This effect was not studied experimentally, but an estimate of the ratio of the quadratic to the linear term was made on the basis of the known fine structure separations. A ratio of the order of parts in 10^5 was found which is within the quoted precision of the measurements.

The effects which influence the g_J values are deviations from L-S coupling, radiative corrections to g_S , configuration interaction, relativistic and diamagnetic effects, and motion of the nucleus. The first two of these have been estimated, ⁽¹⁴⁾ and details will be given below. Configuration interaction with $(3d^4 4s 4p)^7 P$ is certainly present as discussed in the following paper. ⁽³⁾ In addition, the g_J values of that term indicate a breakdown of L-S coupling within the admixed configuration. Thus the combination of configuration and spin-orbit interactions effectively admixes a great many states into $(3d^5 4p)^7 P$ and can drastically affect its g_J values. An accurate evaluation of relativistic and diamagnetic contributions requires a knowledge of the Schroedinger wave functions and cannot be given. Motion of the nucleus results in a correction of a few parts per million to g_L and will be neglected.

In addition to the 7P ground term, the $3d^54p$ configuration possesses a higher lying triplet, ${}^5P_{1,2,3}$. The $J = 2$ and $J = 3$ states of this term are admixed by the spin-orbit operator into the corresponding J states of the ground term. Perturbation theory is used to evaluate the admixture in the following paper. A purely empirical estimate can be made with the use of measured oscillator strengths of intercombination lines whose presence is clear evidence of the breakdown of L-S coupling. In particular, the 7P_3 state combines with the 5S_2 state of $3d^54s$. The wave functions describing the admixture can be written

$$\begin{aligned} |{}^5P_3\rangle &= \alpha |{}^5P_3^0\rangle + \beta |{}^7P_3^0\rangle \\ |{}^7P_3\rangle &= -\alpha |{}^7P_3^0\rangle + \beta |{}^5P_3^0\rangle \end{aligned} \quad (13)$$

The weighted oscillator strengths gf as given in reference (11) can be shown to be proportional to $\frac{1}{\lambda} |\langle a|\vec{P}|b\rangle|^2$ where the matrix element is that of the electric dipole operator between the ground and excited states. Then

$$\begin{aligned} gf({}^5P_3 \rightarrow {}^5S_2) &\propto \frac{1}{\lambda_{5 \rightarrow 5}} \alpha^2 |\langle {}^5P_3|\vec{P}|{}^5S_2\rangle|^2 \\ gf({}^7P_3 \rightarrow {}^5S_2) &\propto \frac{1}{\lambda_{7 \rightarrow 5}} \beta^2 |\langle {}^7P_3|\vec{P}|{}^5S_2\rangle|^2 \end{aligned} \quad (14)$$

where $\lambda_{5 \rightarrow 5}$ and $\lambda_{7 \rightarrow 5}$ are the wavelengths for the quintet and septet transitions respectively, and the coefficients α and β

are those appearing in Eq. (13). The ratio of these equations yields

$$\frac{\beta^2}{\alpha^2} = \frac{\lambda_{7 \rightarrow 5} \text{gf}(^7P_3 \rightarrow ^5S_2)}{\lambda_{5 \rightarrow 5} \text{gf}(^5P_3 \rightarrow ^5S_2)} = 2.81 \times 10^{-3}.$$

Similarly for $J = 2$, $\beta^2/\alpha^2 = 2.20 \times 10^{-3}$. The coefficient β is then 0.053 and 0.047 for the $J = 3$ and $J = 2$ states respectively, in fair agreement with the values predicted by perturbation theory as given in the following paper.

Radiative corrections to g_J can be made by expressing g_J as a sum of g_L and g_S terms and substituting

$$g_S = 2 \left[1 + \frac{\alpha}{2\pi} - 0.328 \frac{\alpha^2}{\pi} \right] = 2(1.0011596)$$

instead of $g_S = 2$. These corrections are listed in Table III. Column one lists the J levels studied. Column two contains the theoretical g_J value with the radiative correction. Column three shows the spin-orbit correction, and column four lists the theoretical g_J . This is compared with the experimental value given in column five. The difference is attributed to relativistic and diamagnetic effects and to configuration interaction.

No detailed discussion will be given here of the measured hyperfine constants as this is the subject of the following paper. It may only be noted that the hyperfine structures are small or zero in all cases, even for the configuration possessing

an unpaired s electron. The results are summarized in Table IV.

ACKNOWLEDGEMENT

The authors gratefully acknowledge the aid and interest of Professor Robert Novick. They wish to thank Messrs. I. Beller, M. Bernstein, C. Dechert, and J. Gorham of the Columbia Radiation Laboratory staff for their prompt and excellent services.

REFERENCES

- (1) C. D. Jeffries and P. B. Sogo, Phys. Rev. 91, 1286 (1953).
- (2) R. W. Terhune, W. J. Lambe, C. Kikuchi, and J. Baker, Phys. Rev. 123, 1265 (1961).
- (3) B. Budick, R. J. Goshen, S. Jacobs, and S. Marcus, Phys. Rev. ___, ___ (196).
- (4) W. J. Childs, L. S. Goodman, and D. von Ehrenstein, Phys. Rev. 132, 2128 (1963).
- (5) A. Lurio, R.L. de Zafra, and R. J. Goshen, Phys. Rev. 134, A1198 (1964).
- (6) P. A. Franken, Phys. Rev. 121, 508 (1961).
- (7) G. W. Series, Reports on Progress in Physics 22, 280 (1959).
- (8) B. Budick, H. Bucka, R.J. Goshen, A. Landman, and R. Novick, Phys. Rev. (to be published).
- (9) B. Budick, A. Lurio, and R. Novick, Appl. Optics 4, 229 (1965).
- (10) M. A. Catalán and P. M. Sancho, An. Soc. Esp. Física y Química (Madrid) 29, 327 (1931).
- (11) M. N. McDermott and R. Novick, Phys. Rev. 131, 707 (1963).
- (12) C. H. Corliss and W. R. Bozman, Experimental Transition Probabilities for Spectral Lines of Seventy Elements, Nat. Bur. Std. Monograph 53, 1962.

(13) The oscillator strengths as given in the Nat. Bur. Std. tables are related to those appearing in Eq. (12) by

$$g_2 f_{\text{NBS}} = g_1 f.$$

(14) R. J. Goshen, Ph.D. Dissertation, Columbia University, 1964.

TABLE CAPTIONS

Table I. Chromium g_J factors in $(3d^5 4p)^7 P_{2,3,4}$.

Table II. Chromium lifetime results.

Table III. Atomic g values; theory and experiment.

Table IV. Experimental hyperfine constants.

Table I

Level	Pure L-S Coupling	rf Spectroscopy Value	Optical Spec- troscopy Value
$J = 4$	1.7500	1.7512 ± 0.0003	1.752
$J = 3$	1.9167	1.9178 ± 0.0002	1.92
$J = 2$	2.3333	2.3351 ± 0.0003	2.334

Table II

Configuration	Level	Experimental		Theoretical
		Optical Spectroscopy (Copper arc)	Hanle Effect	
$3d^5 4p$	7P_4	$(4.53 \pm 3.6) \times 10^{-8} \text{ sec}$	$(3.34 \pm 0.5) \times 10^{-8} \text{ sec}$	Coulomb Approximation (Bates & Damgaard) $1.03 \times 10^{-8} \text{ sec}$
$3d^4 4s 4p$	7P_4	$(10.7 \pm 8.6) \times 10^{-9} \text{ sec}$	$(6.51 \pm 0.9) \times 10^{-9} \text{ sec}$	

Table III

Level	Lande Value with Radiative Correction	Spin-Orbit Correction	Theoretical g_J	Experimental g_J
7P_4	1.751714	0	1.7517	1.7512
7P_3	1.91879	- 0.00070	1.9181	1.9178
7P_2	2.336413	- 0.00110	2.3353	2.3351

Table IV

Configuration	Level	$ a(J) $ in Mc
$3d^5 4p$	7P_4	11.6 ± 0.15
	7P_3	$1.5 \pm 2.0^*$
	7P_2	26.16 ± 0.10
$3d^4 4s4p$	7P_3	70.4 ± 2.6

*This value is an upper limit.

FIGURE CAPTIONS

- Fig. 1. Low-lying energy levels of Cr I.
- Fig. 2. a) Hanle effect in the $(3d^5 4p)^7 P$ term. b) Hanle effect in the $(3d^4 4s 4p)^7 P$ term.
- Fig. 3. Radio-frequency coil for double resonance.
- Fig. 4. High-field double resonance in even isotopes of chromium.
- Fig. 5. High-field double resonance in $(3d^5 4p)^7 P_3$ of Cr^{53} .
- Fig. 6. High-field double resonance in $(3d^5 4p)^7 P_4$ of Cr^{53} .
- Fig. 7. High-field double resonance in $(3d^5 4p)^7 P_2$ of Cr^{53} .

CHROMIUM I

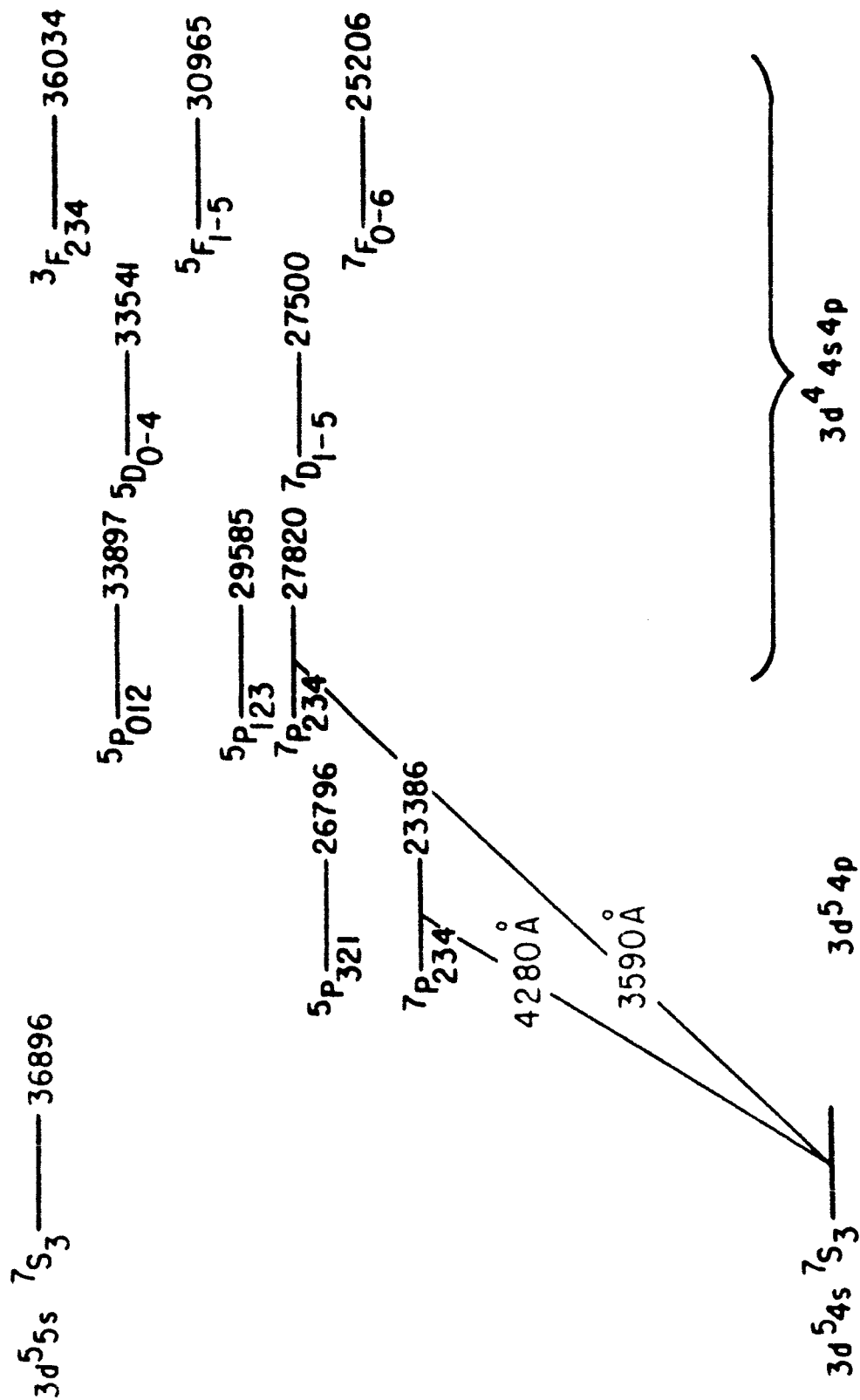
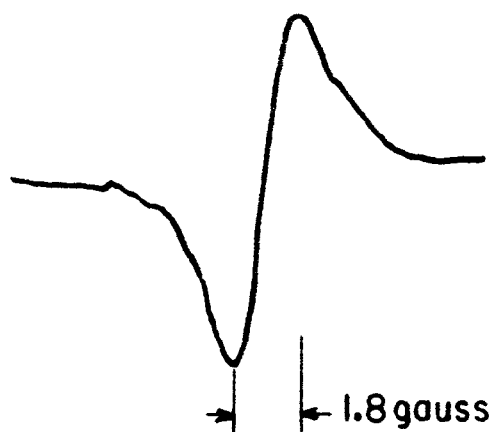


FIG. 1.

a)



b)

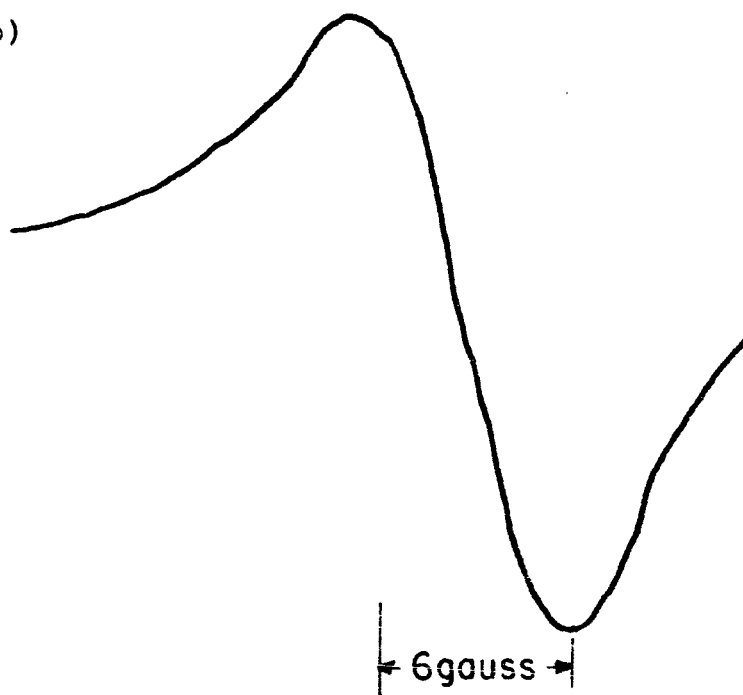


FIG. 2.

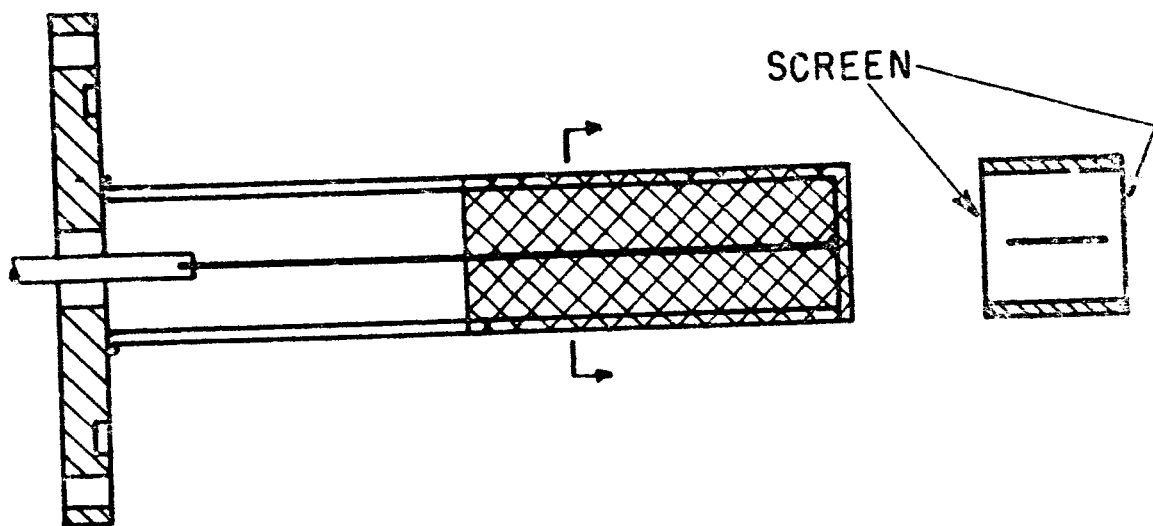


FIG. 3.

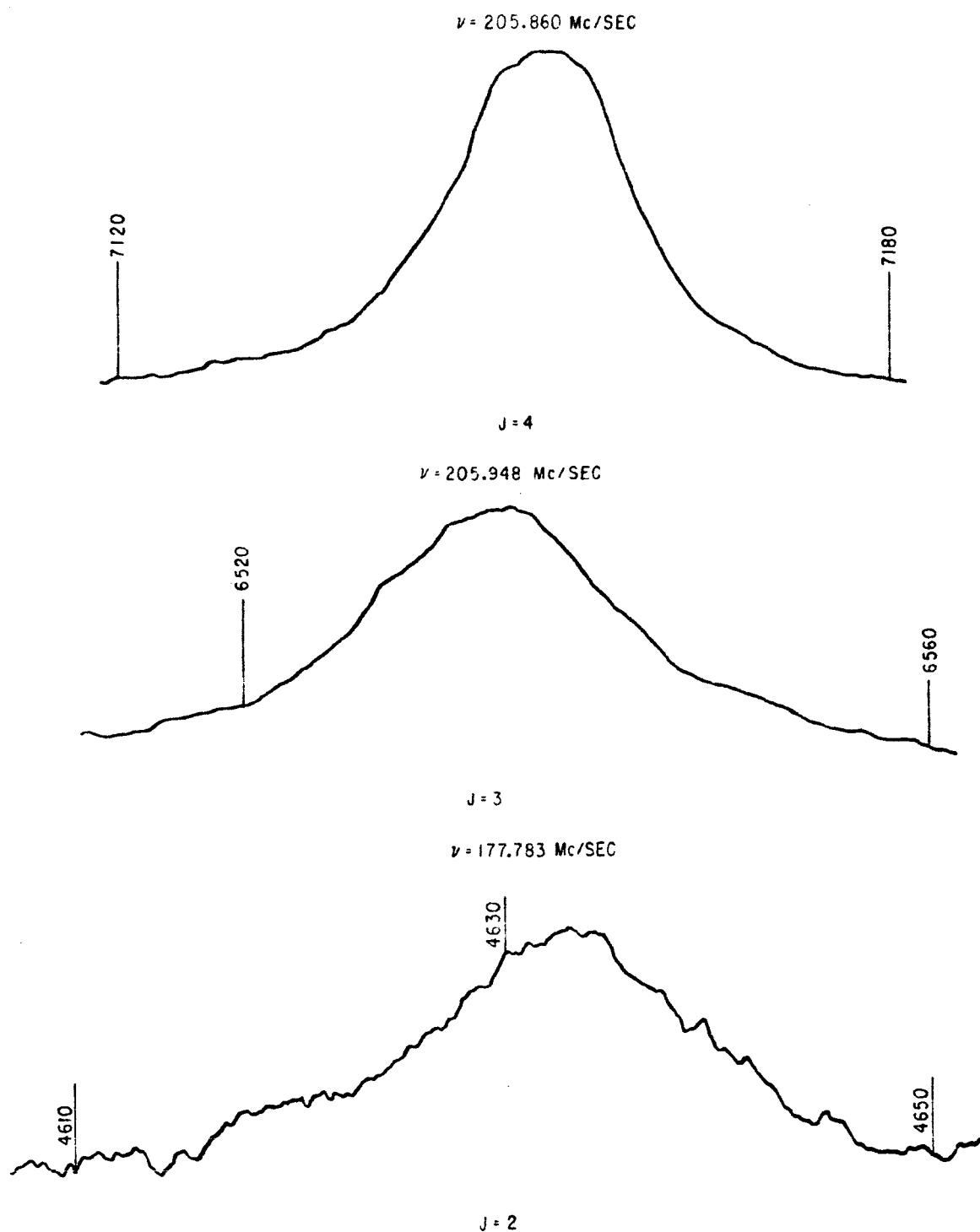


FIG. 4.

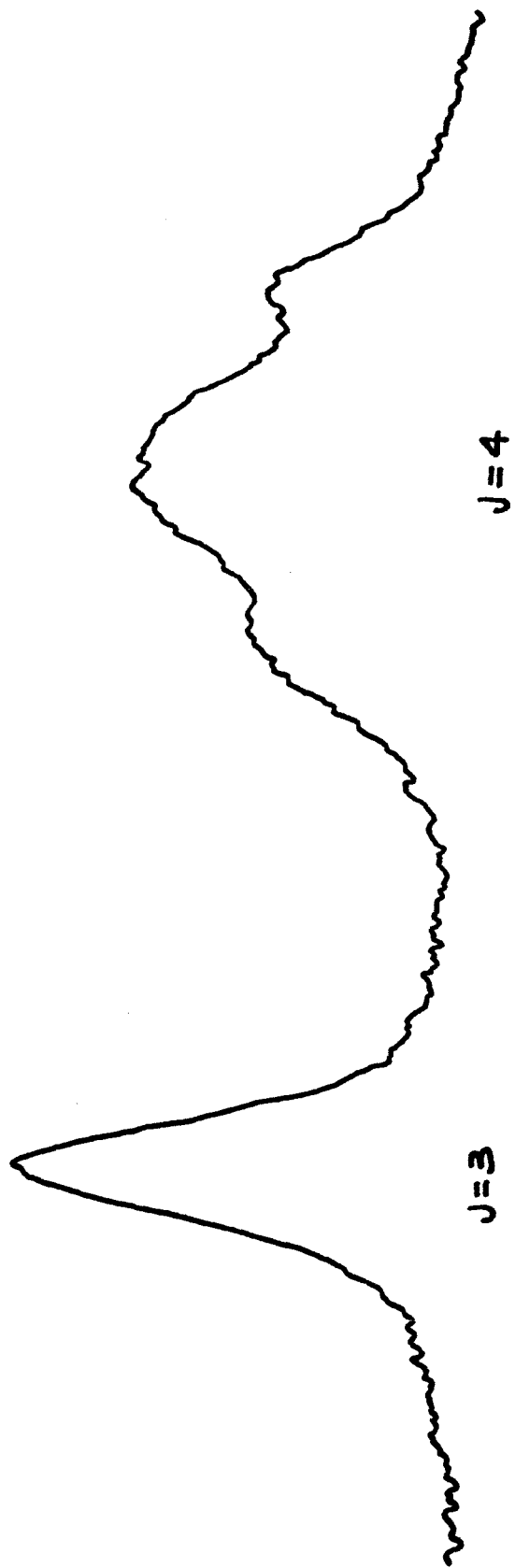


FIG. 5.

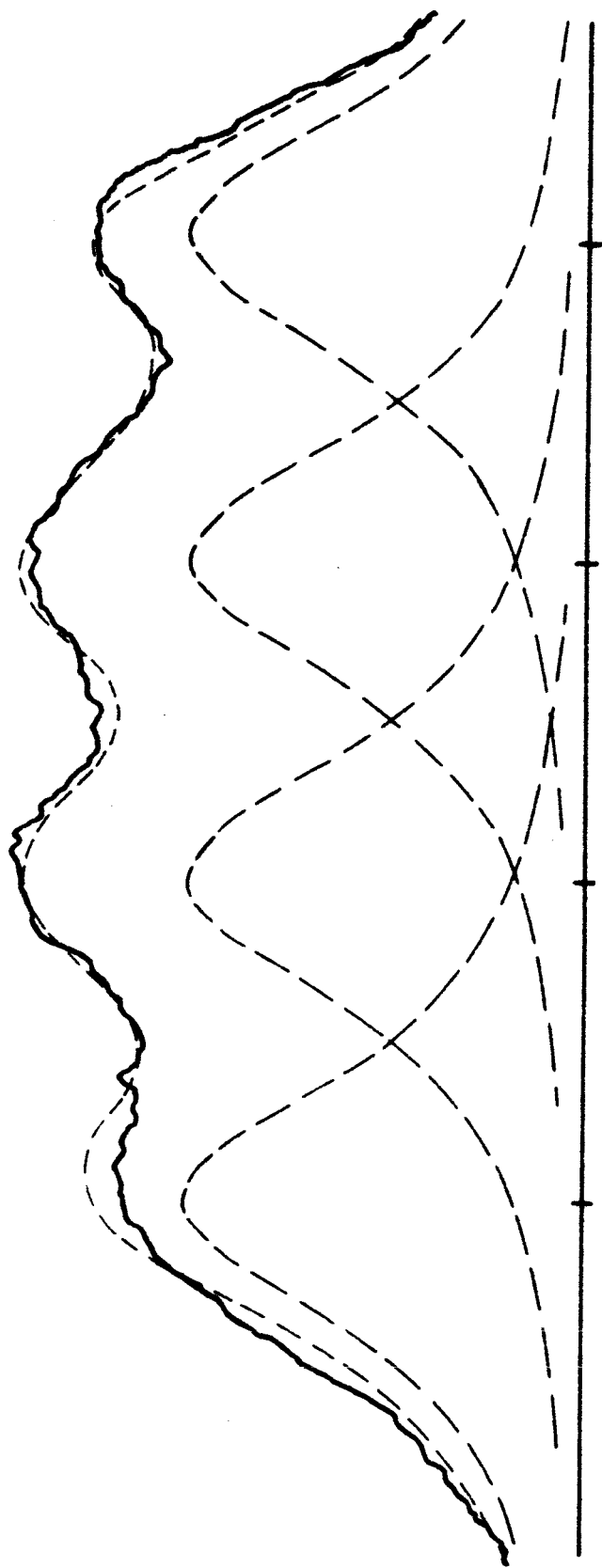


FIG. 6.

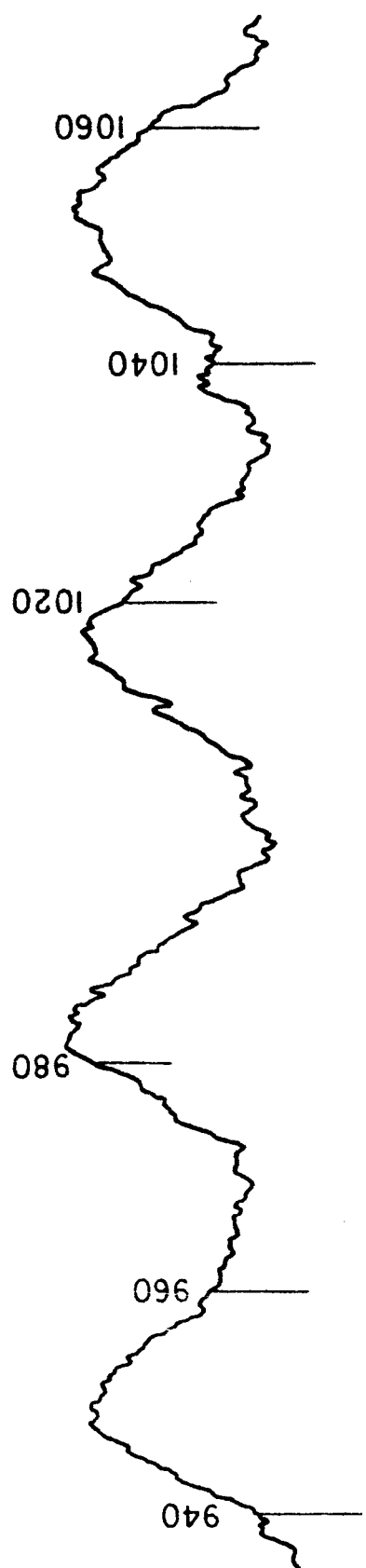


FIG. 7